Planetary and Space Science 125 (2016) 72–79

Contents lists available at ScienceDirect

Planetary and Space Science

journal homepage: www.elsevier.com/locate/pss

MESSENGER X-ray observations of magnetosphere–surface interaction on the nightside of Mercury

S.T. Lindsay [a,*], M.K. James [a], E.J. Bunce [a], S.M. Imber [a,b], H. Korth [c], A. Martindale [a], T.K. Yeoman [a]

[a] University of Leicester, Department of Physics & Astronomy, University Road, Leicester LE1 7RH, UK
[b] Department of Atmospheric, Oceanic and Space Sciences, University of Michigan, Ann Arbor, MI, USA
[c] Johns Hopkins University Applied Physics Laboratory, Laurel, MD, USA

ARTICLE INFO

Article history:
Received 11 December 2015
Received in revised form
3 March 2016
Accepted 4 March 2016
Available online 18 March 2016

Keywords:
Mercury
Magnetosphere
Electrons
XRS
X-ray fluorescence
MESSENGER

ABSTRACT

The recently completed MESSENGER mission to Mercury has detected X-ray fluorescence events on the nightside surface of the planet, induced by the precipitation of electrons. We expand upon previously reported catalogues of such events, using a filter based on elemental fluorescence lines to construct a catalogue covering the full five years of the MESSENGER mission. We find that the locations of the majority of these events are ordered in two clear latitudinal bands on the dawn side of the planet centred at ~50°N and ~20°S. Electron precipitation is implied to be either stable or occurring repeatedly on timescales of up to several minutes, long in relation to characteristic times of the Mercury magnetospheric environment. Conversely, X-ray fluorescence events are observed on only ~40% of MESSENGER orbits, although we note that some events are inevitably lost during the filtering process. We suggest that the regions of most intense precipitation are determined by the location of the relevant magnetic field line footprints on the surface. We are able to place speculative limits on the energies of electrons precipitating in this manner based on fluorescence lines in the observed X-ray spectra. The poleward boundaries of the regions of most intense precipitation are found to be collocated with the open-closed field line boundary. We use a magnetic field model to trace field lines from these fluorescence sites to implied locations of origin in the magnetotail.

1. Introduction

The MESSENGER (MErcury Surface, Space ENvironment, GEochemistry, and Ranging) spacecraft was launched in August 2004 and achieved Mercury orbit on 18 March 2011 (Solomon et al., 2007). The orbital mission at Mercury lasted four years, before the spacecraft impacted the planetary surface on 30 April 2015. During this time, significant advances have been made in our understanding of Mercury's environment.

MESSENGER's orbit was highly elliptical, with periapsis (h_p=200–500 km) at low altitude over the north pole and apoapsis high above the southern hemisphere (h_a=15 000 km, τ=12 h or h_a=12 750 km, τ=8 h dependent upon mission phase).

The MESSENGER X-Ray Spectrometer (XRS) was an X-ray fluorescence spectrometer consisting of three gas proportional counter (GPC) detectors (Schlemm et al., 2007), using a balanced filter method (Adler et al., 1972a,b) to separate the Kα fluorescence lines of the major rock-forming elements Mg (1.25 keV), Al (1.49 keV) and Si (1.74 keV). One GPC (GPC1-Mg) was equipped with a 4.5 μm Mg filter, the second (GPC2-Al) with a 6.3 μm Al filter, and the third (GPC3-UN) was unfiltered. The Mg and Al K-shell absorption edges (1.30 keV and 1.56 keV respectively) cause significant absorption within the respective filters across a small energy range. The differences between the spectra recorded by each of the three GPCs can thus be used to separate these three fluorescence lines.

XRS was nominally nadir-pointing with a 12° hexagonal field of view (FOV) with a triangular transmission function as a function of off-axis angle. XRS was paired with the Solar Assembly for X-rays (SAX), a solar monitor consisting of a Si PIN diode mounted on the spacecraft sunshield, used to monitor the incident X-ray spectrum (Schlemm et al., 2007).

Results from MESSENGER orbital operations in 2011 included the detection of X-ray fluorescence taking place on the nightside surface of Mercury (Starr et al., 2012), which was attributed to the impact of energetic particles on the planetary surface. Starr et al. (2012) characterises the illuminating particles as electrons with a kappa distribution in energy peaking at $0.8 < E < 1.4$ keV, and demonstrates sensitivity to the composition of the surface, producing elemental

* Corresponding author.
E-mail address: s.t.Lindsay@le.ac.uk (S.T. Lindsay).

http://dx.doi.org/10.1016/j.pss.2016.03.005

abundance estimates for Mg, Al, S and Ca. Here, we extend the catalogue of nightside fluorescence events to cover the whole mission and discuss the location of the fluorescence sites and the implications for processes within Mercury's magnetic field.

2. Identification and characterisation of surface sites of electron-induced fluorescence

The existing catalogue of nightside electron-induced fluorescence events in 2011 was presented by Starr et al. (2012), who do not state how the events in question were identified. We have developed an automated filter to isolate candidate events over the full MESSENGER mission from March 2011 to April 2015, based on the detection of Si and/or Ca-Kα fluorescence from the unlit planetary surface. This filter applies a series of criteria to each XRS calibrated data record (CDR) as follows:

1. Rejects records with a low total count rate at any of the three GPCs ($< 2\ s^{-1}$ over whole spectrum).
2. Uses a peak finder (Dimeo, 2004) to check that there are more than zero peaks in the GPC spectrum. If no peaks are found, record is rejected.
3. Attempts a least-squares fit of a Gaussian curve to the GPC3 spectrum at 1.74 keV (Si-Kα).
4. If fitted peak has a maximum in the range $1.5 < E < 1.95$ keV, a width in the range $0.9 < \mathrm{FWHM} < 1.4$ keV and a coefficient of determination $R^2 > 0.8$ (all criteria are selected empirically), then record is flagged as containing Si fluorescence.
5. If record is flagged, attempts to fit a peak to the GPC3 spectrum at 3.69 keV (Ca-Kα).
6. If fitted peak has a maximum in the range $3.4 < E < 3.8$ keV, a width in the range $1.4 < \mathrm{FWHM} < 1.8$ keV and a coefficient of determination $R^2 > 0.9$ (all criteria are selected empirically), then record is flagged as containing Ca fluorescence.
7. If evidence exists of instrumental self-fluorescence in the Mg and Al filters (Mg/Al count rate at Mg/Al-filtered detector elevated above Mg/Al count rate at unfiltered detector) record is unflagged for both Si and Ca fluorescence.
8. If telemetry point FOV_STATUS (available in XRS CDR telemetry) indicates the instrument footprint is sunlit or entirely off planet, record is unflagged for both Si and Ca fluorescence. This is done to reject both solar-induced X-ray fluorescence and observations from astrophysical X-ray sources.

Si fluorescence is an ideal criterion for the filtering process as the energy required to excite it is low, and Si is expected to be present on the surface in large quantities with a near-isotropic distribution across the planet (Weider et al., 2015).

As described above we also produced a second catalogue based on the detection of Ca-Kα fluorescence in order to isolate events in which the illuminating flux is implied to contain a higher energy component. As with Si, Ca should be ubiquitous on the surface of the planet, with the average Ca/Si ratio being around 0.15, although more variation in Ca concentration is expected (Weider et al., 2015).

Fig. 1 shows an example spectrum collected by XRS at 15:23 UTC on 4 June 2012, with an integration time of 40 s. This record was selected by both the Si and Ca fluorescence filters described above. The spectra in Fig. 1 have been smoothed using a top hat filter 23 bins ($\sim$880 eV) in width to match the energy resolution of 880 eV FWHM at the Fe-K line (Schlemm et al., 2007). The strong Ca peak at 3.7 keV can be seen at all three GPCs, along with the Mg/Al/Si peak complex at $\sim$1.2–1.8 keV, which is observed as a single peak due to the energy resolution of the instrument. While Mg and Al peaks at the Mg and Al filtered GPCs may be indicative

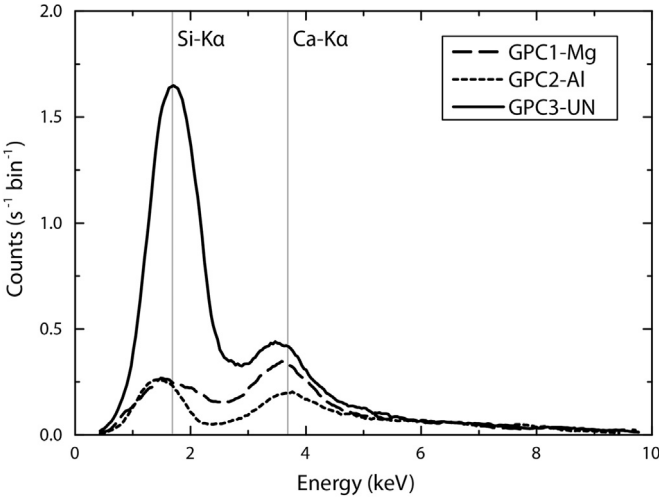

Fig. 1. Example XRS spectrum produced by electron-induced surface fluorescence, observed at 15:23 UTC on 4 June 2012; the original data have been smoothed using a top hat adjacent-averaging filter 23 bins in width. Si-Kα and Ca-Kα fluorescence energies are indicated.

of self-fluorescence, the presence of a strong peak at the unfiltered detector implies surface fluorescence, possibly from all three elements, although Si will usually be the strongest. Si/Mg/Al and Ca are not present in the unfiltered detector in areas vulnerable to self-fluorescence and thus we can be confident that their detection here is due to surface fluorescence.

Here we define a fluorescence "event" as made up of one or more contiguous "records" which are selected by the filter. Each record represents a single XRS integration time, which can vary between a minimum of 20 s and a maximum of 450 s depending on orbit and solar activity. Each event can be several records long, although the length of an event in terms of records does not necessarily reflect its length in time due to this wide variation in integration time.

The timestamps of records in the Si- and Ca-filtered electron-induced fluorescence catalogues were used as inputs to an analysis in SPICE (Acton, 1996), which retrieved the locations of the intersection of vectors describing the six corners of the XRS FOV, thus locating the region of the surface contributing to the observed fluorescence signal.

Subsequently, the spatial location of the XRS FOV on the planetary surface for each event was used as an input to a magnetic field model. A number of models of Mercury's magnetosphere exist (e.g. Luhmann et al., 1998; Sarantos et al., 2001; Korth et al., 2004; Alexeev et al., 2008). The magnetic field model used in this study is the KT14 model (Korth et al., 2015). The KT14 model consists of a number of modules, much like its counterparts made for Earth's magnetosphere (e.g. Tsyganenko, 1995, 2002a,b, 2013; Tsyganenko and Sitnov, 2005). The magnitude and morphology of each of the modules, or field sources, has been determined empirically and contained within a realistic magnetopause (Shue et al., 1997; Johnson et al., 2012). The KT14 model enables the tracing of field lines into the magnetotail without encountering unrealistic O-lines (Korth et al., 2014) like those which are found in the paraboloid model of Alexeev et al. (2008). This allows us to map events observed in the magnetosphere along field lines to the surface of Mercury, or from Mercury to a location within the magnetosphere – such as the magnetic equatorial plane.

The KT14 model was used to trace the implied magnetic field line associated with each fluorescence event back from its magnetic footprint (assumed to be collocated with the intersection of the XRS boresight with the planetary surface at the time of the event) to the magnetic equator. This analysis assumes that the